The SEARCH 2004-2006 project

1 Introduction

SEARCH (Seismic Experiment in the Aysén Region of CHile) is a collaborative project between the Universities of Cambridge (UK), Tokyo (Japan) and Concepción (Chile) with the principal objective of determining the plate geometry and mantle structure to the east of the Chile triple junction, especially in the region where the 6 Ma old ridge segment has been subducted. This involved running a network of 60 seismometers in the region between the dates of January 2004 and February 2006, with regular visits to service the seismometers and remove the data.

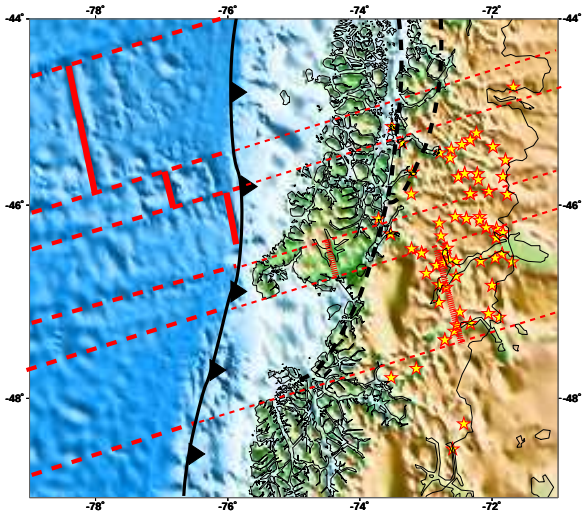

Figure 1. Tectonic setting in the region of the Chile triple junction, known as the Aysén region of Chile, showing the spreading centres (thick red lines), fracture zones (dashed red lines), subducted spreading centres (dashed thick red lines), subduction trench (black line, triangles indicate subduction direction), the Liquiñe-Ofqui fault system (dashed black lines), and the seismicity from 1964-2004 from the EHB catalogue (red/white/black circles). Stars denote station locations. Places of interest in the region are labelled 1-9. 1 - Triple junction; 2 - Taitao peninsula; 3 - Golfo de Penas; 4 - Hudson volcano; 5 - Lago General Carrera / Buenos Aires; 6 - northern ice field; 7 - southern ice field; 8 - the 3 Ma subducted ridge; 9 - the 6 Ma subducted ridge.

2 Equipment used and timeline of the deployments

The seismological equipment used in this fieldwork was provided by Seismic Equipment Infrastructure in the UK (SEIS-UK). SEIS-UK is the seismic node of the Geophysical Equipment Facility, funded by the National Environmental Research Council (NERC) in the UK. In total 60 seismometers of three different types were used, which were manufactured by Güralp Systems:

- **CMG-3T**. 14 CMG-3T broadband seismometers were installed in January 2004. These have a near-flat response to velocity from 120 s to 50 Hz.

- **CMG-40T**. 6 CMG-40T intermediate band seismometers were installed in January 2004. These have a near-flat response to velocity from 30 s to 100 Hz.
- **CMG-6TD**. 40 CMG-6TD intermediate band sensors were installed in January/February 2005. These have a near-flat response to velocity from 30 s to 100 Hz.

The seismometers were serviced every four months and removed in January/February 2006. A map of the station locations is shown in Figure 1.

3 Seismicity of the Aysén region

The temporary network of the SEARCH experiment enabled the first study of the local seismicity throughout the whole of the Aysén Region. Seismic events of sufficient magnitude to be recorded teleseismically by permanent arrays are extremely rare and therefore do not give much information on the seismicity or geometry of this subduction zone.

The continuous data recorded by the network was scanned visually, and the times of coherent signals arriving at more than one station in the network, and their approximate lengths, were noted. This had the advantage of detecting a more complete dataset; and also anomalous signals, which did not have a typical P- and S-wave structure, could be noted and kept in the dataset at this stage. Finally, the arrival times of these coherent signals were compared to a global catalogue of events. If the signals were found to come from a teleseismic source they were removed from the dataset. A final catalogue of 1293 local events for the time period 2004:022 to 2006:026 was produced. Event files were produced in the Seismic Analysis Code (SAC) format and archived.

The program used to locate the events was HYPOINVERSE-2000. As the crustal velocities in this region are not well constrained, several different velocity models were used with HYPOINVESE-2000 to obtain the earthquake locations. The final velocity model used to obtain the locations presented here was based on Robertson Maurice et al. (2003) which was based on regional waveform inversion to obtain the crust and upper mantle structure in southern South America.

Of 1293 local events detected by the scanning process, 789 had sufficient data quality to have a P phase pick at a minimum of three different stations. This is the minimum requirement for location by triangulation. Of these 789 events, 684 could be located well with an RMS residual of less than 0.5 seconds.The event distribution is displayed in Figure 3. The majority of the events lie at depths less than 30 km, located between longitudes 75.5°W and 72.5°W. Further east from this region, sparse shallow events exist up to ∼71°W, lying between latitudes of 46°S and 47.5°S, and one final M_L 2.1 event at 46.7°S 70.2°W. However, the regions to the north and south of these events do not show seismicity, even though they are only ∼100 km from the network. The extent of the events appears to correlate with the coastline. Areas offshore, including the Golfo de Penas, do not show seismicity. However, the position of the coastline also is at a distance from the network where it becomes difficult to locate local events, so it is expected that offshore events, especially near to the subduction trench, will not be picked up by this network, especially if they have a low magnitude.

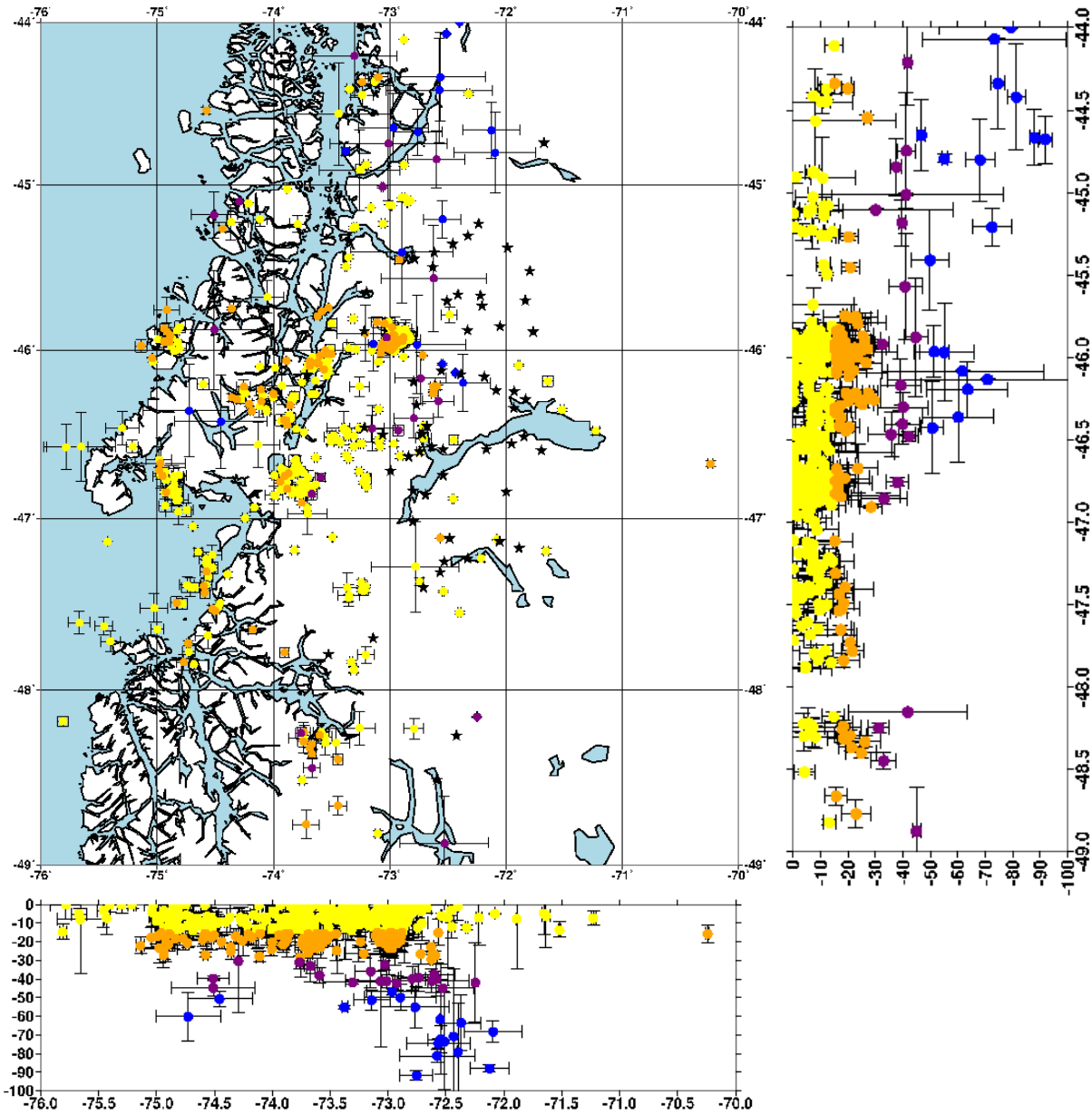

Figure 2. The local locations obtained in this study. The data presented here is a map view of the field area, with E-W and N-S cross sections displayed at the sides of the map, where the depth scale is in kilometres. The stations used in the location appear as black stars, and the events as circles. The events are colour coded depending on their depth - Yellow events lie between 0 and 15 km depth, orange between 15 and 30 km, purple between 30 and 45 km, and blue between 45 and 90 km. The 95% error bars calculated by the location program are displayed for each event.

Several of these shallow events occur close to the predicted position of the Liquiñe-Ofqui fault that runs through the region. However, as these lie outside the network, the error in the locations does not clarify whether the events are on this fault or are associated with other crustal deformation and simply coincide with the position of this fault. The deeper events are represented on Figure 2 as purple (30-45 km depth) or blue (45-90 km depth). These events are poorly located, as evidenced by the error bars. These events show a highly attenuated waveform, with the energy arriving between frequencies of 1 to 5 Hz. Often the picking errors were large and it was impossible to pick the S arrival from such events, indeed 23 out of 26 events located below 40 km depth did not have any S picks.

4 Teleseismic travel time tomography

Travel time tomography uses the arrival times of waves travelling through the Earth to produce an image of the seismic wave velocity structure of the interior. This study used teleseismic P and S waves to generate the upper mantle structure underneath the field area in the form of velocity, or slowness (reciprocal of velocity), perturbations by comparing the relative arrival times between rays arriving at different locations.

In total 173 events were identified that were suitable for P-wave tomography. These events provided 2534 P-wave arrival times for use in the P tomographic inversion. 124 events provided 1544 S-wave arrival times for the S tomographic inversion. A multi-channel cross correlation method was used to measure the relative arrival times for this study. From checkerboard tests, the P velocity structure has a maximum resolution of $\sim$40 km and the S velocity structure has lower resolution, with structures on a minimum length scale of $\sim$90 km resolvable.

The P velocity structure presented in Figure 3 shows a large difference between the northern and southern parts of the region. To the north, a $\sim$100 km thick fast anomaly exists which dips away from the subduction trench; this is likely to be related to the subducting Nazca plate. As the age of this plate at the subduction trench decreases, the fast anomaly migrates further from the trench suggesting that the Nazca plate subducts at a low angle over a larger distance before the subduction angle steepens. Where the 6 Ma subducted ridge segment is predicted to lie there is a region of lower velocities between $\sim$250 and $\sim$100 km depth, and no fast region associated with a subducting slab is present.

If the subduction geology changes depending on the age of the subducting plate, then due to the abrupt changes in the age of the sea floor at the subduction trench from north to south there should be clearly distinct changes in the positions of the subducted segments of the Nazca plate on profiles which run perpendicular to the fracture zones. The best-resolved profile underneath the network is profile 7 (shown in Figure 4); and this indeed shows distinct regions of $\sim$100 km thick fast anomalies which start off shallow further south (near the centre of the profiles) and then get progressively deeper to the north. Also, the profile shows a slow velocity zone underneath these fast regions as was seen in the profiles B, D and F.

The S velocity structure has lower resolution but the low velocity zone associated with the 6 Ma subducted ridge segment is still visible. Although they cannot be combined directly to give details about the percentage anomalies in Poisson's ratio, the S

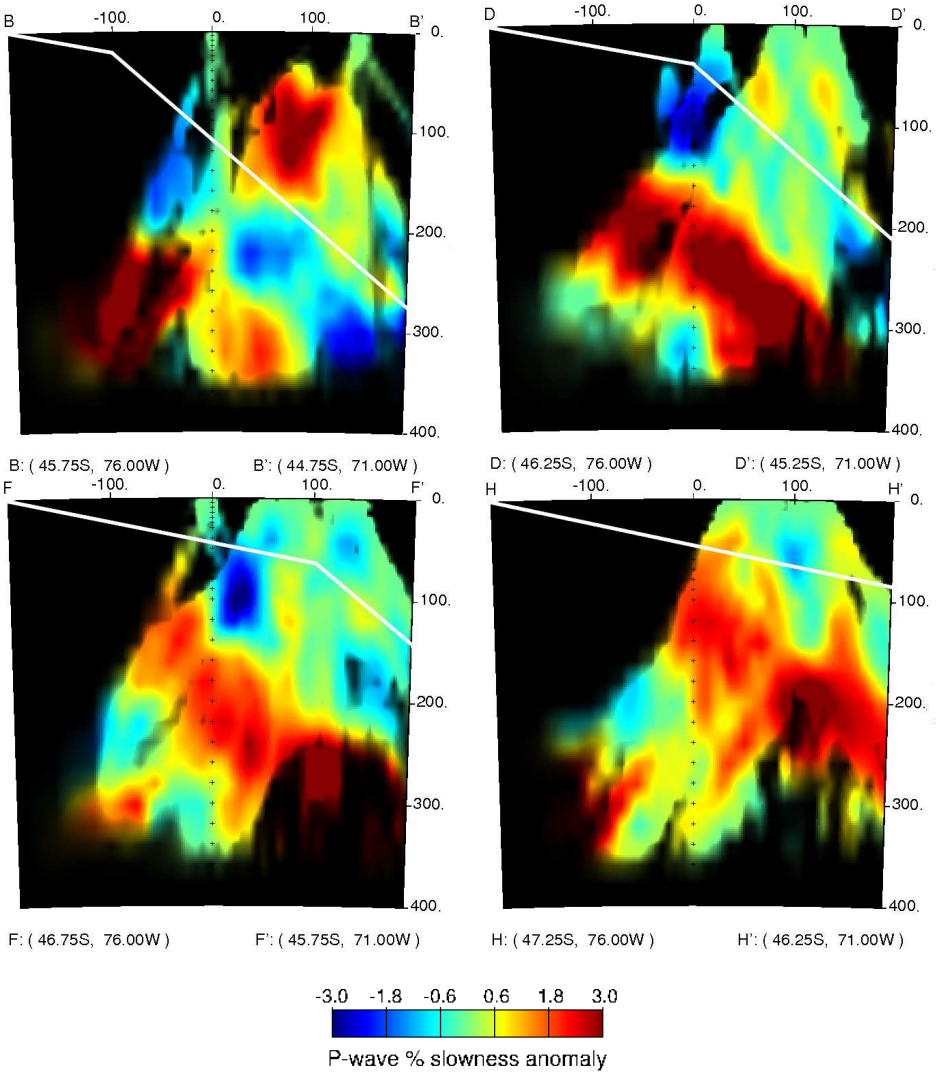

Figure 3. Selected P tomography profiles running parallel to the offshore transform faults. The location of the Chile Trench is approximately at 76°W, at the top-left corner of these profiles. On the profiles B, D and F an additional white line is added showing a rough predicted position of the top of the subducting oceanic plate. The slowness anomaly is presented as a percentage deviation from the reference IASP91 velocity model, with red regions being slower than the reference and blue regions being faster than the reference model. Areas of low ray coverage, less than 0.01 km^{-2}, are shown in black or with reduced brightness at the edge of the illuminated region. For the positions of these profiles with respect to the subduction setting refer to Figure 1.

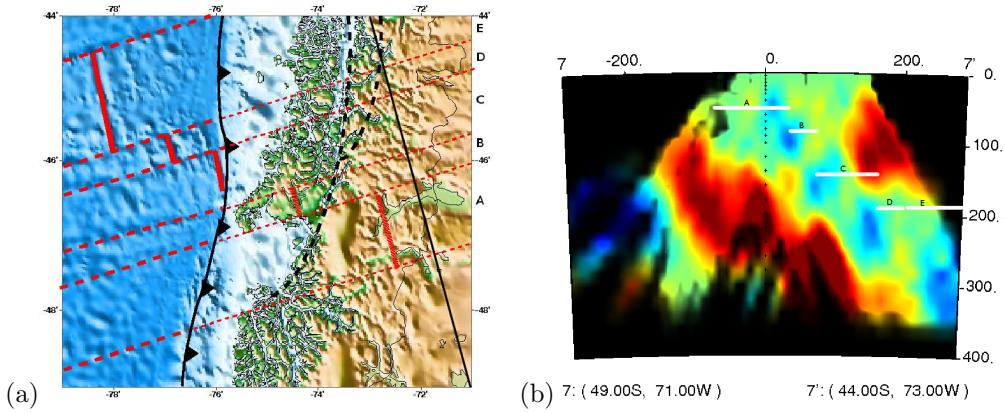

Figure 4. (a) The location map, labelling the different subduction situations. The age of the Nazca plate at the trench being A: ∼-6 Ma; B: ∼-3 Ma; C: ∼0 Ma; D: ∼2 Ma; E: ∼4 Ma. Here negative values mean that the mid-ocean ridge subducted that many years ago. Profile 7 is also marked on this map for reference as a black solid line. The tectonic features are the same as in Figure 1. (b) P tomography profile 7, annotated with the predicted positions of the top of the subducting Nazca plate segments from the model discussed as horizontal white lines. The scale is the same as for the previous plot, Figure 3.

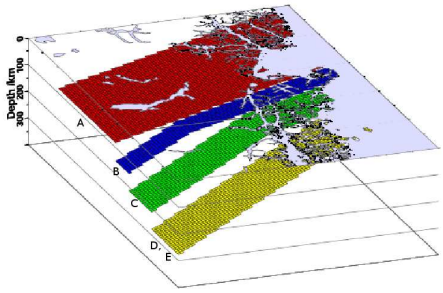

Figure 5. The proposed tectonic model based on the P tomography interpretation. The region is now viewed from the northeast, at an oblique angle. The model shows the different slab segments (shown in different colours) which subduct at an angle of 11° initially before changing to a steeper angle of 40°, however, the position of the 'hinge point' between these two subduction angles varies depending on the age of the subducting slab.

tomographic model compliments the P tomographic model well and is in agreement with the conclusions drawn from the P structure within the limits of the resolution. The S-wave tomography is particularly sensitive to the thermal effects of ridge subduction in this region, and better resolution is necessary to draw definite conclusions about the structure of the mantle due to ridge subduction. A diagram of the slab structure beneath the region based on the P-wave tomography analysis is shown in Figure 5.